Electronic Supplementary Material (ESI) for Journal of Materials Chemistry A.

Supporting Information

Graphene Oxide- and Low-Density Polyethylene Based Highly Sensitive Biomimetic Soft Actuators Powered by Multiple Clean Energies of Humidity and Light

Yiwei Zhang, Ruiqian Wang, Wenjun Tan, Lianchao Yang, Xiaolong Lv, Xiaodong Wang, Feifei Wang and Chuang Zhang*

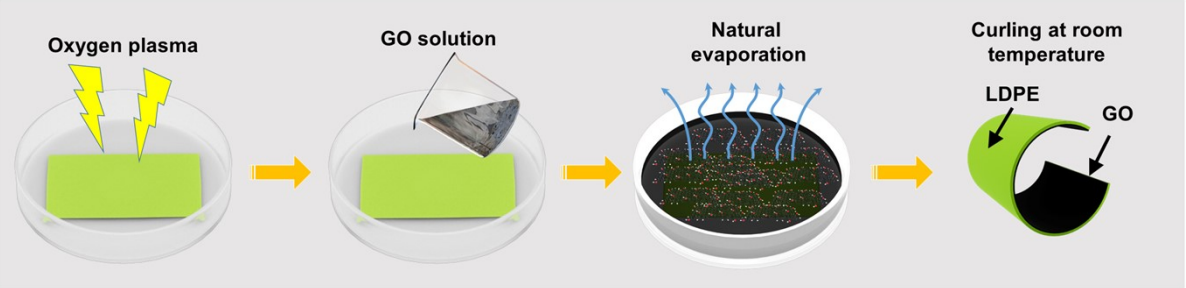

Fig. S1 Manufacturing process of the GO/LDPE actuator.

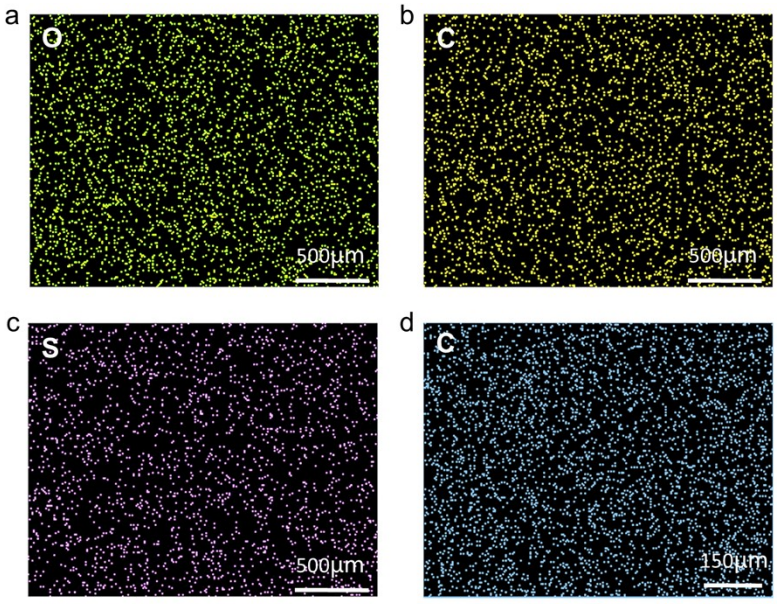

Fig. S2 Characterization of actuator surface elements. (a) Distribution of oxygen on the surface of GO. (b) Distribution of oxygen on the surface of GO. (c) Distribution of sulfur on the surface of GO. (d) Distribution of carbon on the LDPE surface.

Fig. S3 Shape of the GO/LDPE film before heat treatment.

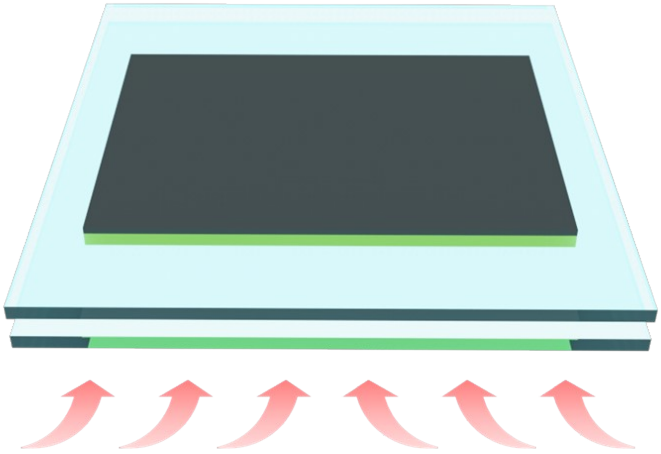

Fig. S4 Schematic diagram of heat treatment.

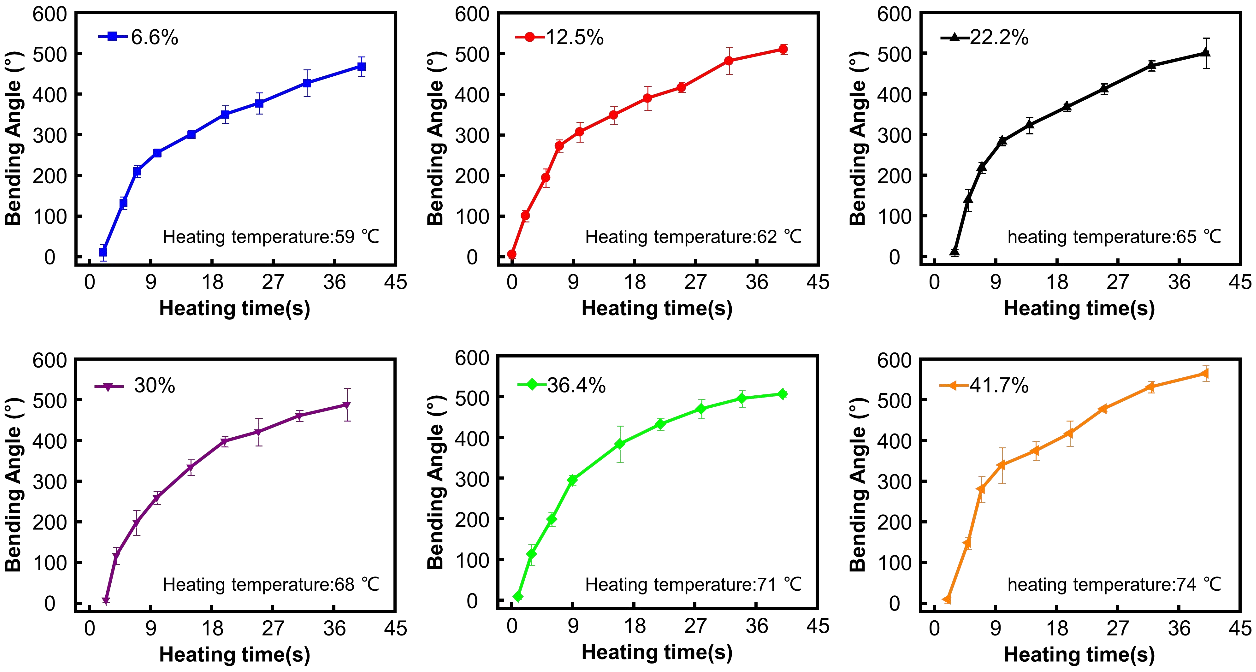

Fig. S5 Thermal adjustment curve of the GO/LDPE actuator based on different GO contents.

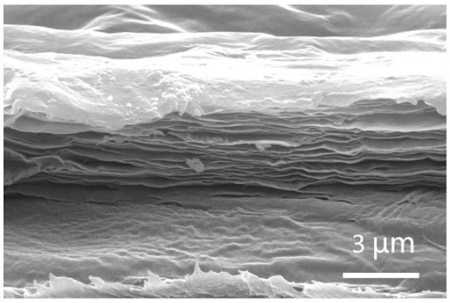

Fig. S6 Cross-sectional SEM image of the GO-22.2/LDPE actuator after the cycling tests for 40 cycles.

Tab.S1 Performance comparison of soft actuator with light and humidity response characteristics

Response type	Materials	Structure	Thickness（μm）	Max bending angle (°) (Sitimuli intensity)	Velocity of bending (°/s)	Ref.
Light	MXC/PDMS	Bilayer	90	219 (NIR 500 mW cm^{-2})	25	1
	TDW/LDPE	Bilayer	/	160 (NIR 120 mW cm^{-2})	5.33	2
	GO	Monolayer	/	183 (NIR 600 mW cm^{-2})	36.68	3
	I-MXene/PE	Bilayer	~3	700, (NIR 200 mW cm^{-2})	333.3	4
	WSG	Bilayer	150	80 (NIR 970 mW cm^{-2})	15.22	5
	CE/HEPCP/MW CM-2CNT (LHM)	Monolayer	/	180 (NIR 320 mW cm^{-2})	90	6
	Ti_3C_2Tx/PET	Bilayer	/	90, (NIR 500 mW cm^{-2})	14.62	7
	MXene/LDPE	Bilayer	45.6	390 (NIR 172 mW cm^{-2})	50.57	8
	GO/EC	Bilayer	40	430 (NIR 140 mWcm^{-2})	44	9
Humidity	MXene/CNF/PDA	Monolayer	24	176 (△RH 40%)	106.25	10
	PEG-COF	Bilayer	80	120 (△RH 34%)	5.22	11
	RO/GM	Bilayer	/	300 (Steam on the water)	5	12
	GO/ SU-8	Bilayer	15	357 (△RH 74%)	13.73	13
	CNF/GO/CNT	Monolayer	/	180 (△RH 40%)	225	14
	GO	Monolayer	20-100	600 (△RH 74%)	85.7	15
	CMC/MXene/Al 3+	Monolayer	12	180 (△RH 80%)	92.1°/s	16
	GO	Monolayer	~55	1100 (△RH 60%)	47.6	17
Light/ humidity	GO/WAX	Bilayer	14.41	360 (NIR 78mW cm^{-2})	225	18
				360 (△RH 20%)	90	
	CNT–Nafion/PE	Bilayer	50	220 (NIR 100 mW cm^{-2})	71.88	19
				1031 (△RH 30%)	/	
	PG/Nafion	Bilayer	48.1	301, (NIR 1200mW cm^{-2})	/	20
				343 (△RH50%)	/	
	GO/MXene	Bilayer	4.5	116 (NIR 140 mW cm^{-2})	55.5	20
				730 (△RH74%)	15	
	PDMS-CNT/CS	Bilayer	301.9±7.2	384 (NIR 500 mW cm^{-2})	18.45	21
				391 (△RH 92%)	12.5	
	PVDF–CB/PEA/PAM	Bilayer	150	199 (NIR 250mW cm^{-2})	331.67	22
				292 (△RH 55%)	18.25	
	GO/PET	Bilayer	100	130 (NIR 400 mW cm^{-2})	25	23
				300	/	

			(△RH 80%)		
RCF/PTFE	Bilayer	/	360 (NIR300 mW cm^{-2})	36	24
			720 (△RH 25%)	11.08	
MGO/BOPP	Bilayer	11.71	750, (NIR 160 mW cm^{-2})	6.67	25
			275 (△RH 65%)	/	
GO/PPy	Bilayer	25.2	120 (IR 83mW cm^{-2})	40.13	26
			360 (△RH 19%)	40	
GO/LDPE	Bilayer	37	500 (NIR 40 mW cm^{-2})	110	This work
			500 (△RH 35%)	69.2	

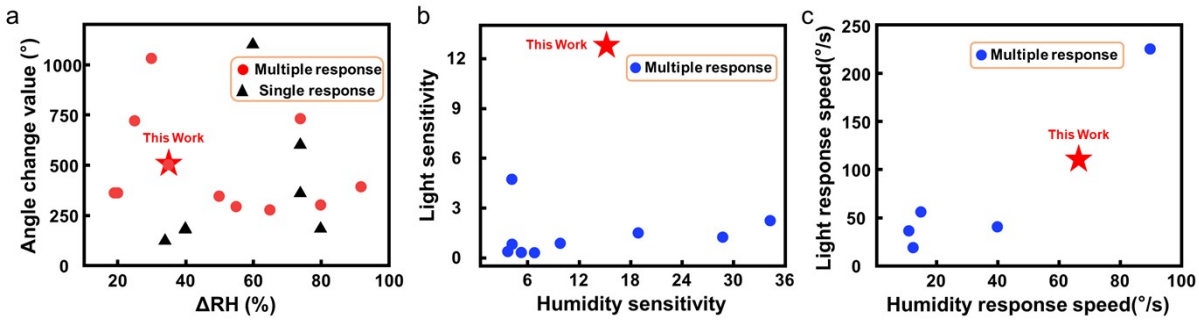

Fig. S7 Comparison of response characteristics of actuators based on different materials: (a) Comparison of humidity performance of actuators with single or multiple response characteristics. (b) Comparison of light sensitivity and humidity sensitivity of actuators with multiple response characteristics, humidity sensitivity is the maximum bending angle divided by the desired △RH; light sensitivity is the maximum bending angle divided by the required illumination intensity. (c) Comparison of light response speed and humidity response speed of actuators with multiple response characteristics.

Movie S1: Inchworm-inspired soft robot crawls directionally on A4 paper.

Movie S2: Environmental simulation test, inchworm-inspired soft robot crawls on leaves.

Movie S3: Adaptive soft gripper grabs and releases balls, capsules and flowers under humidity control.

Movie S4: Adaptive soft gripper grabs and releases balls, capsules and flowers under the sequential control of humidity and NIR light.

Movie S5: Rotating robot with four rotors rotates under the synergistic stimulation of humidity and NIR light.

Movie S6: Rotating robot uses the co-stimulations of humidity and NIR light to drive the boat forward.

References:

1. H. Q. Li, Z. Wu, Y. Q. Xing, B. J. Li and L. Liu, *Nano Energy*, 2022, **103**, 107821.
2. D. T. Zhang, K. Yang, X. Y. Liu, M. Luo, Z. Li, C. Z. Liu, M. Li, W. M. Chen and X. Y. Zhou, *Chem. Eng. J.*, 2022, **450**, 138013.
3. M. C. Weng, Y. W. Xiao, L. Q. Yao, W. Zhang, P. D. Zhou and L. Z. Chen, *Acs Appl. Mater. Inter.*, 2020, **12**, 55125-55133.
4. Y. Hu, L. L. Yang, Q. Y. Yan, Q. X. Ji, L. F. Chang, C. C. Zhang, J. Yan, R. R. Wang, L. Zhang, G. Wu, J. Sun, B. Zi, W. Chen and Y. C. Wu, *Acs Nano*, 2021, **15**, 5294-5306.
5. Z. W. Su, Y. J. Zhao, Y. Q. Huang, C. Y. Xu, X. L. Yang, B. R. Wang, B. B. Xu, S. Q. Xu and G. X. Bai, *Nano Res.*, 2022, **16**, 1313-1319.
6. Z. H. Yu, Y. M. Wang, J. Q. Zheng, S. Sun, Y. Fu, D. Chen, W. H. Cai, D. Wang, H. M. Zhou and D. Q. Li, *Acs Appl. Mater. Inter.*, 2022, **14**, 16649-16657.
7. K. H. Yang, C. C. Fu, C. W. Li, Y. J. Ye, M. Ding, J. H. Zhou, Y. Bai, F. L. Jiao, J. Ma, Q. H. Guo and M. C. Weng, *Sens. Actuators, A*, 2022, **341**, 113553.
8. X. J. Luo, L. L. Li, H. B. Zhang, S. Zhao, Y. Zhang, W. Chen and Z. Z. Yu, *Acs Appl. Mater. Inter.*, 2021, **13**, 45833-45842.
9. D. Gao, M. F. Lin, J. Q. Xiong, S. H. Li, S. N. Lou, Y. Z. Liu, J. H. Ciou, X. R. Zhou and P. S. Lee, *Nanoscale Horiz.*, 2020, **5**, 730-738.
10. L. Y. Yang, J. Cui, L. Zhang, X. R. Xu, X. Chen and D. P. Sun, *Adv. Funct. Mater.*, 2021, **31**, 2101378.
11. T. H. Mao, Z. Y. Liu, X. X. Guo, Z. F. Wang, J. J. Liu, T. Wang, S. B. Geng, Y. Chen, P. Cheng and Z. J. Zhang, *Angew. Chem. Int. Edit.*, 2022, **62**, e202216318.
12. M. M. Kong, H. J. Li, Y. Liang, K. Cheng, X. Zhou, X. J. Song, Z. H. Yang, J. M. Xu and L. Zhao, *Sens. Actuators, B*, 2023, **380**, 133390.
13. J. N. Ma, Y. L. Zhang, D. D. Han, J. W. Mao, Z. D. Chen and H. B. Sun, *Natl. Sci. Rev.*, 2020, **7**, 775-785.
14. J. Wei, S. Jia, J. Guan, C. Ma and Z. Q. Shao, *Acs Appl. Mater. Inter.*, 2021, **13**, 54417-54427.
15. Y. L. Zhang, Y. Q. Liu, D. D. Han, J. N. Ma, D. Wang, X. B. Li and H. B. Sun, *Adv. Mater.*, 2019, **31**, 1901585.
16. J. Wei, S. Jia, C. Ma, J. Guan, C. X. Yan, L. B. Zhao and Z. Q. Shao, *Chem. Eng. J.*, 2023, **451**, 138565.
17. M. T. Wang, Q. C. Li, J. X. Shi, X. Y. Cao, L. Z. Min, X. F. Li, L. L. Zhu, Y. H. Lv, Z. Qin, X. Y. Chen and K. Pan, *Acs Appl. Mater. Inter.*, 2020, **12**, 33104-33112.
18. Y. Dong, L. Wang, N. Xia, Y. Wang, S. J. Wang, Z. X. Yang, D. D. Jin, X. Z. Du, E. W. Yu, C. F. Pan, B. F. Liu and L. Zhang, *Nano Energy*, 2021, **88**, 106254.
19. L. F. Chang, D. P. Wang, Z. S. Huang, C. F. Wang, J. Torop, B. Li, Y. J. Wang, Y. Hu and A. Aabloo, *Adv. Funct. Mater.*, 2023, **33**, 2212341.
20. J. H. Kim, J. B. Pyo and T. S. Kim, *Adv. Mater. Interfaces*, 2020, **7**, 2001051.
21. H. Xu, X. Z. Xu, J. W. Xu, S. P. Dai, X. Dong, F. Han, N. Y. Yuan and J. N. Ding, *J. Mater. Chem. B*, 2019, **7**, 7558-7565.
22. J. J. Li, M. L. Wang, Z. P. Cui, S. Y. Liu, D. Y. Feng, G. K. Mei, R. Zhang, B. G. An, D. Qian, X. Zhou and Z. F. Liu, *J. Mater. Chem. A*, 2022, **10**, 25337-25346.
23. K. H. Yang, Z. D. Tang, Y. J. Ye, M. Ding, P. Q. Zhang, Y. K. Zhu, Q. H. Guo, G. Q. Chen and M. C. Weng, *J. Appl. Polym. Sci.*, 2022, **139**, e52014.
24. Y. N. Li, J. Wang, H. X. Li, L. L. Huang, L. H. Chen, Y. H. Ni and Q. H. Zheng, *Appl. Surf. Sci.*, 2022, **572**, 151502.
25. L. Li, G. W. Jia, W. W. Huang, J. Y. Zhou, C. X. Li, J. X. Han, Y. Zhang and X. J. Zhou, *Sens. Actuators, A*, 2023, **351**, 114149.

26. Y. Dong, J. Wang, X. K. Guo, S. S. Yang, M. O. Ozen, P. Chen, X. Liu, W. Du, F. Xiao, U. Demirci and B. F. Liu, *Nat. Commun.*, 2019, **10**, 4087.